

## Laser eco-printing technology for silk fabric patterns

Jinxiang Chen<sup>1, a</sup>, Chuang Meng<sup>2</sup>, Juan Xie<sup>1</sup>, Le Pan<sup>1</sup>, Dong Zhou<sup>3</sup> & JunNan Chen<sup>3</sup>

<sup>1</sup> International Institute for Urban Systems Engineering & School of Civil Engineering, Southeast University, Nanjing 210096, China

<sup>2</sup> Art and Design Academy, Zhejiang Sci-Tech University, Hang Zhou 310018, China

<sup>3</sup> Chengxian College, Southeast University, Nanjing 210000, China

*Received 25 September 2013; revised received and accepted 4 August 2014*

In this study, silk microstructures and the yellowing mechanism have been investigated to develop laser eco-printing technology for silk patterns (SLEP). Carbonized microstructures are divided into bar-shaped clots and sludge materials with small holes. The former are created by the initial pyrolysis (melting) of raw silk on the fabric surface; and the latter are the combined result of the development of the former during in-depth printing. The chemical composition and structure of the thermogravimetry/pyrolysis features of raw silk under different atmospheres have also been investigated. The yellowing mechanism of silk after SLEP and the feasibility of SLEP are demonstrated by analyzing its thermogravimetry/pyrolysis properties. Silk fabric patterns printed by SLEP exhibit yellow chromaticity with 10% lightness, and their boundaries are clear and distinct.

**Keywords:** Inkless eco-printing, Pyrolysis, Silk, SEM microscopy

### 1 Introduction

The popularity of raw silk, a natural fibre often referred to as the queen of fibres, is rivaled by man-made, synthetic, and other functional fibres. However, silk fabrics are still widely favored by consumers because of their unique characteristics, such as their elegance and excellent texture<sup>1-6</sup>. Many silk fabrics have interesting or colorful designs that make them beautiful and lively. To date, such patterns can be created using methods such as hand painting, color printing<sup>7,8</sup>, spraying<sup>9,10</sup>, weaving<sup>11,12</sup>, or embroidery<sup>13</sup>. Each of these methods has its own advantages. For example, hand painting can produce unique, colorful patterns, whereas weaving can produce highly reproducible patterns at a high production speed. However, the common feature of each method is the need for dye—all of these methods require the dyeing of raw silk or fabrics or the spraying of dye onto silk fabrics. Therefore, the use of dye not only makes fibre production processes more complex and costly but also makes these processes more harmful to the environment and even to human health<sup>14, 15</sup>.

Recently, the researchers proposed an innovative concept involving heat-induced eco-printing (HIEP) on ordinary paper without the use of toner or ink<sup>16-18</sup>.

This technology uses the yellowing discoloration of plant fibres and eliminates the environmental pollution caused by the ink used in the printing industry<sup>19</sup>. By testing and analyzing the pyrolysis volatiles of printing paper, they proved that the volatiles produced after HIEP did not include any carcinogens, and hence, HIEP was found to be an environment friendly technology<sup>20-22</sup>.

In this study, a new silk laser eco-printing (SLEP) technology based on heat-induced inkless eco-printing has been developed. This paper presents a comprehensive exploration of the microstructure produced by SLEP, its thermogravimetric (TG)/pyrolysis properties, the yellowing discoloration mechanism, and printing effects.

### 2 Materials and Methods

For printing of silk fabric patterns (color block) and chromaticity measurement, laser ablation was performed using a laser (maximum power of 30 W, resolution of 0.025 mm), a high speed stepper motor (maximum line speed of approximately 1 m/s), and control software. The silk fabric used in this study was plain crepe satin (68.9 g/m<sup>2</sup>, raw silk: 22.2-24.4 dtex). Preliminary experiments were performed using six samples, three line speeds of printing (300, 600, and 900 mm/s), and two different power levels (Power 1 and Power 2). For each sample, five

<sup>a</sup>Corresponding author.  
E-mail: chenjpaper@yahoo.co.jp

color blocks (3 mm width and 5 mm length) were produced, and the lightness ( $L^*$ ) and chromaticity ( $x, y$ ) at two points on each color block were measured using a color luminance meter (TOPCO, BM-5A). The total sample capacity of each group was 10.

The microstructure of the aforementioned color blocks was observed by an ultra plus field emission scanning electron microscope (SEM, Carl Zeiss NTS GmbH, Oberkochen, Germany).

TG and differential thermal analysis (DTA) curves of the silk fabric were measured using an STA 409 P C/PG (NETZSCH, Germany) calorimeter in  $N_2$  and air at a heating rate of  $10^\circ\text{C}/\text{min}$ .

### 3 Results and Discussion

#### 3.1 Microstructure Type and Formation Process

Figure 1 shows the microstructure of the color blocks. The laser power used to produce the materials on the left is lower than those on the right, and the laser power and print speed increase from top to bottom. For comparison, Figs 2(a) and (b) show

SEM images of materials produced without heat-induced printing, whereas Figs 2(c) and (d) show partially magnified images of a typical carbonized microstructure. Figure 1 clearly shows that the carbonized microstructures after SLEP are similar to those of sludge materials (star); there are many small holes (circle) and bar-shaped clots (triangle).

While printing at low power [Fig 1 (a), (c) and (e)], more intact fibres remain, as also shown for the two samples printed at higher speeds [Figs 1(c) and (e), wide arrow]. This result demonstrates that samples are not easily carbonized when using a high printing speed and short heating time. Figures 1(a), (c) and (e) show the formation of sludge with many clots and the interweaving of the fibres, whereas the right side of Figs 1(b), (d) and (f) show the formation of sludge materials, which are essentially integrated together to form sludge materials with many small holes. This result demonstrates that at the same speed, a higher power leads to a higher degree of fibre carbonization and the formation of more sludge material. The

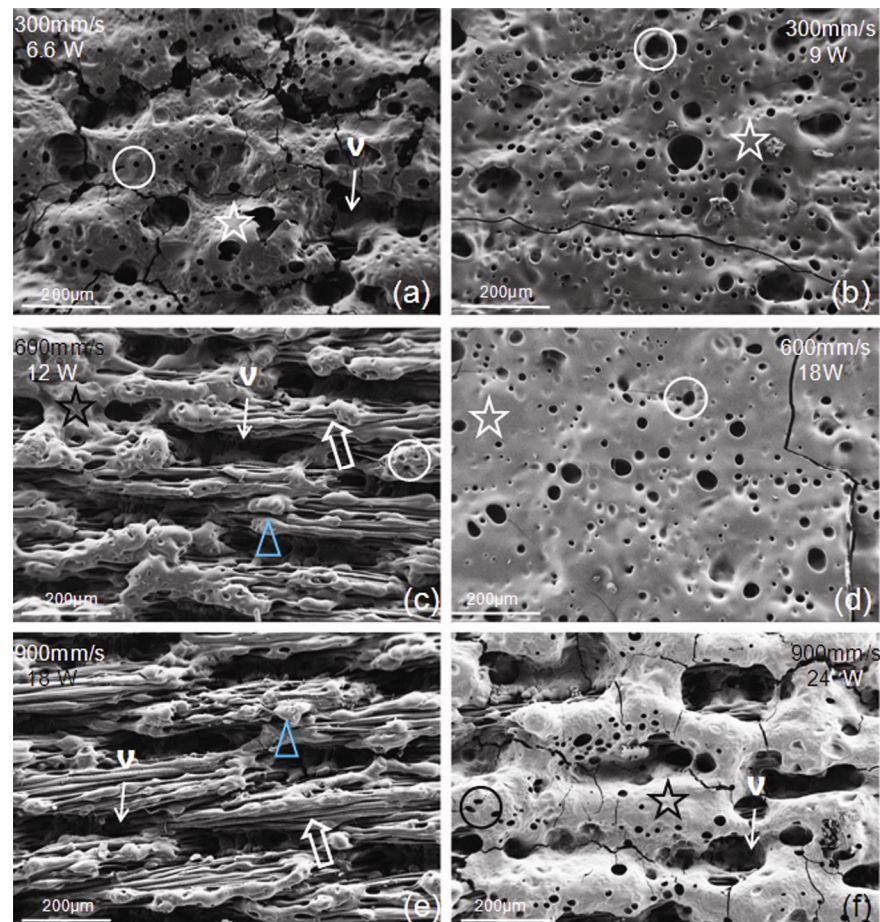


Fig. 1—Microstructures of the silk fabric after SLEP with different print speeds and laser power settings (a-f) [v—interspaces, arrows—fibre, circle—small holes, triangle—clot material, and star—sludge]

degree of carbonization is influenced more strongly by power than by print speed [Figs 1(b), (d), and (f)]. In contrast, clots are primarily distributed over samples treated with low laser power [Figs 1(c) and (e)]. Cracks in sludge materials are not generated by laser printing; they are generated by exogenic action during the preservation process. The interspaces among the clots [Figs 2(a),( c), and (e)] are not generated by carbonization decomposition but by the weaving of warp and weft yarn, as shown in the structural images of the unprocessed silk [(Figs 2(a) and (b)]. Therefore, the carbonization of silk fabric under laser irradiation is presumed to occur as follows. Firstly, the raw silk on the silk fabric surface begins to soften and bulges to form clots. Then, as the laser power or print time increases, degradation occurs along the vertical and horizontal directions until the sample finally becomes an even sludge material with small holes.

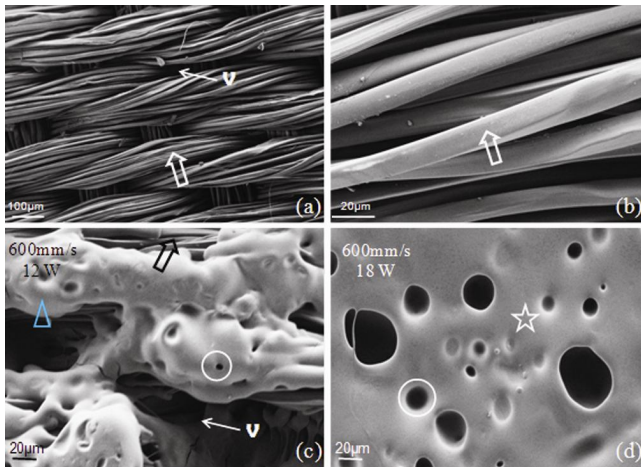


Fig. 2—Silk fabric structure before laser printing (a, b), its magnified image (b), and a typical carbonized microstructure after SLEP at the different laser power settings (c, d) [the marks are the same as in Fig. 1]

**3.2 Thermogravimetric/Pyrolysis Properties of Silk Fabric and Influencing Factors**

Figures 3a and b show the TG and DTA curves of the silk fabric obtained in nitrogen and air, respectively. Although the critical temperature, speed, and rate of weight loss vary between the two different environments, their TG curves can be divided into five stages. Their temperature and weight loss at each critical point (Cp 1-4) are shown in Table 1. In stage I, weight loss occurs slowly with a ratio of 7% due to water evaporation<sup>23, 24</sup>. From stage II (with a critical point of ~ 280°C) to stage V, weight loss occurs rapidly [Fig. 3(a)] due to the pyrolysis of raw silk<sup>25, 26</sup>. This finding is consistent with the TG results reported by Zhang for raw silk in nitrogen<sup>27, 28</sup> (Table 1). This consistency suggests that the critical points in the TG curves are dominated by the composition and structure of raw silk. Raw silk (mulberry silk) is composed of eighteen amino acids<sup>29</sup>, that primarily include glycine (43%), alanine (32%), serine (15%), and tyrosine (12%)<sup>30</sup>. The remaining contents are present in quantities of less than 2%, except for valine (3%), and half of the other amino acids are present in quantities of less than 1%. Amino acids themselves

Table 1—Temperature and mass loss shown by the main peaks in the TG curves

Property	Cp 1	Cp 2	Cp 3	Cp 4
<b>N<sub>2</sub> (by Zhang<sup>27</sup>)</b>				
Temp., °C	280	320	450	-
<b>N<sub>2</sub></b>				
Temp., °C	285	340	455	710
Mass loss, %	94	60	46	35
<b>Air</b>				
Temp., °C	280	350	510	600
Mass loss, %	94	66	36	15

Cp1-Cp4 are the temperature and weight loss at each critical point as shown in Fig. 3.

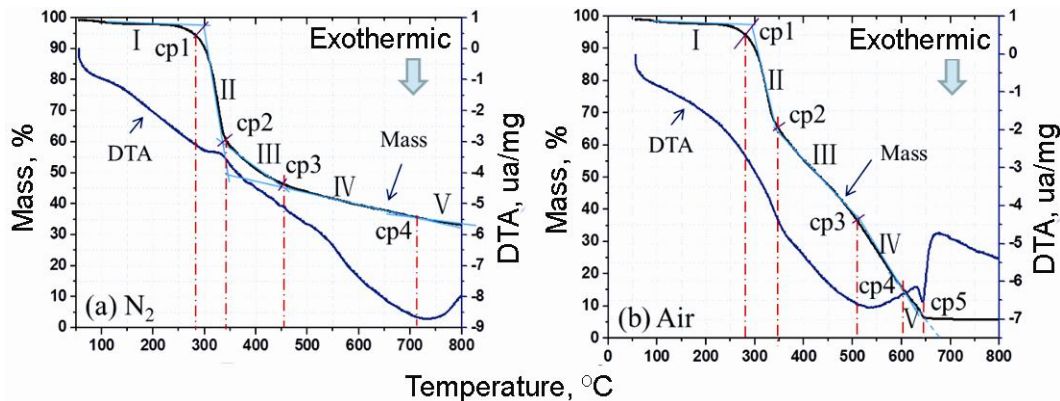


Fig. 3—TG and DTA curves of silk fabric (a) nitrogen and (b) air

are colorless crystals with melting points between 200°C and 300°C. Raw silk is a fibrous protein. The eighteen amino acids that comprise raw silk form a peptide chain (H chain) with a high molecular weight and one to three peptide chains with a low molecular weight. The H chain typically appears in the form of a  $\beta$ -sheet or  $\alpha$ -helical structure. Each amino acid in raw silk is integrated into a chain formed by large molecules with a melting point of  $\sim 300^\circ\text{C}$ . However, Fig. 3(a) shows the phenomenon of rapid weight loss beyond  $\sim 280^\circ\text{C}$  (Stages II-V). Different weight loss rates observed from the second stage to the fifth stage are primarily dominated by the structural forms of raw silk. Raw silk is comprised of a crystallization region, a noncrystallization region, and a transition region<sup>31</sup>. The crystallization region is primarily composed of 3:2:1 ratio of glycine, alanine, and serine with small side chains. The noncrystallization region is composed of amino acids with large side chains or polar radicals. The per cent crystallinity of raw silk is 40-50%. Therefore, the pyrolysis of raw silk in the second stage could occur in the noncrystallization region. Pyrolysis during crystallization differs from that in the transition regions, based on the heating atmosphere used. In nitrogen, a pyrolysis residue content above 32% persists in the final material, even in temperatures up to 800°C. However, in air, the final material shows a residue content of less than 5% when heated to temperatures below 650°C. This phenomenon occurs because, as compared to a nitrogen atmosphere, oxidation or hydrolysis accompanies pyrolysis in air, which accelerates the speed at which the critical temperature is reached as well as the rate of weight loss (Table 1 and Fig. 3). Therefore, the speed of pyrolysis and the weight loss of raw silk are largely accelerated by a combination of temperature and a high oxygen content.

### 3.3 Printing Effects and Yellowing and Discoloration Mechanism

Figure 4(a) shows the lightness  $L^*$  of each sample together with the color blocks. Figure 4b shows several printed samples. Figure 5 shows the carbonized microstructure of raw silk near the print boundary. Figure 4(a) shows that the  $L^*$  values ranged from 10 to 35 under the experimental conditions and are approximately 10 at Power 2, i.e. 90% of black 0 (the  $L^*$  value of full white is 100). The chromaticity results show that the values of  $x$  range from 0.42 to 0.44, whereas the values of  $y$  range from 0.38 to 0.40 and are primarily distributed in the range of yellow chromaticity without any large fluctuations. Differences in the color blocks processed at different powers are primarily due to different lightness  $L^*$  values [Fig. 4(a)]. The carbonized microstructure along the print boundary shows several swollen fibres (Fig. 5), and the transition region from the non-printed to the normally carbonized material is extremely narrow. This effect is due to the small diameter of the laser spot used and the concentration of the laser energy at the printed points. Thus, good printing effects are obtained under these experimental conditions despite the disparity in chromaticity and lightness values (Fig. 4) between the print samples.

As discussed above, the degree of weight loss and pyrolysis (change in composition and structure) of silk fabric vary due to different thermal effects and the atmospheric conditions (Fig. 3). This result is due to the use of a laser with a thin light beam and concentrated energy and because the printing time is extremely short (the duration of laser ablation was less than 1 ms for each print point) with SLEP technology. In other words, SLEP has features that include a high concentration of energy and a short heating time. Therefore, although the experiment was

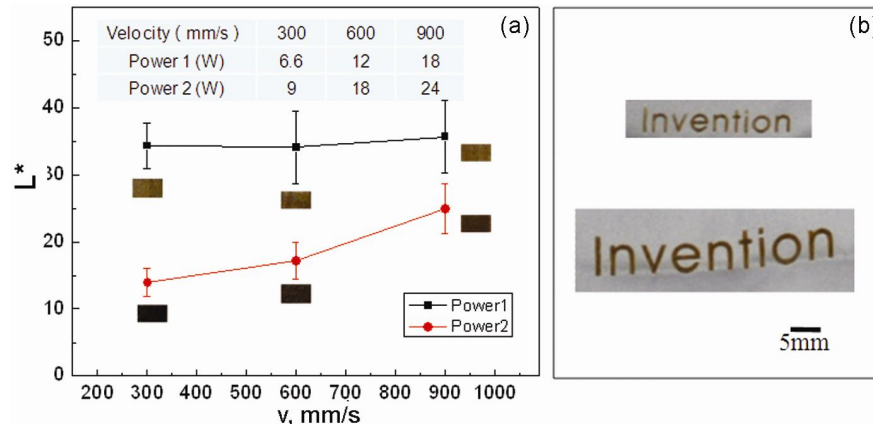


Fig. 4—Laser ablation conditions and printing effects (a) color blocks and their lightness  $L^*$  values, and (b) printed samples

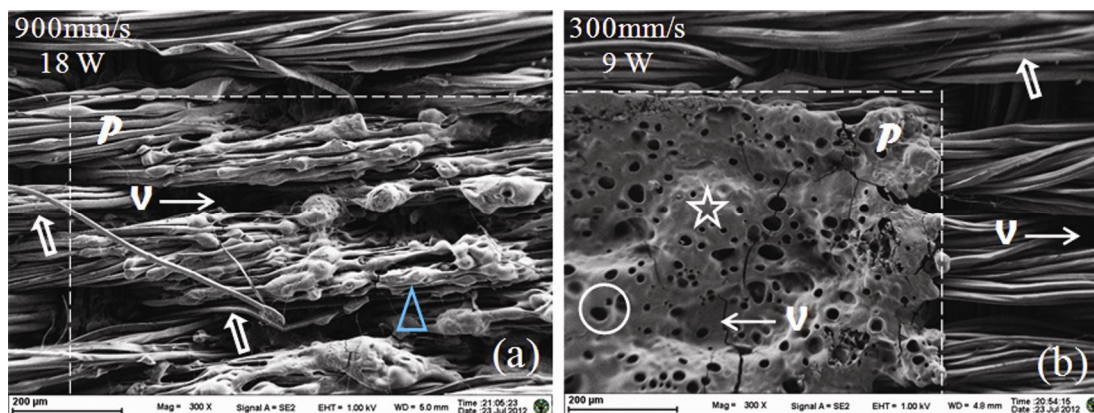


Fig. 5—Carbonized microstructure of silk fabric on the lettered boundary after SLEP (a) Power 1 and (b) Power 2 [white dotted line divides the print lines; the letter P denotes the printed side; the other marks are the same as in Fig. 1]

performed in air, a condition in which silk generally undergoes oxidation and pyrolysis (pyrolysis), fibrous proteins on the surface of the silk fabric that were irradiated (printed) melted immediately (Fig. 1) regardless of the composition or higher order structure in the crystallization and non-crystallization regions due to the high laser energy density. Even peptide chains, composed of large molecules in raw silk fibres formed by amino acids and all types of polar radicals in amino acids, are directly destroyed. Moreover, as expected, protein fibres are carbonized at high temperatures. Hence, although there are differences in both the parameters of the SLEP process and the microstructure of the silk fabric after printing (Fig. 1), the differences primarily concern the quantity (area and depth) of the carbonized protein fibres and are not essentially distinct, because the laser parameters used in this study are determined based on preliminary experiments. Thus, from a macroscopic view, good printing effects are obtained even though there are differences in lightness and chromaticity. For example, the lightness values are approximately 10 under the three conditions involving high power. The lightness value is near the 0 value of black, as high as 90%. In addition, analysis of the microstructures of the silk fabric before and after printing (qualitative analysis) indicates that carbonization occurs primarily on the surfaces of the silk fabric (warp or weft) and that the carbonization depth is approximately 1/10 - 1/4 of the fabric thickness (Fig. 5, estimated by visual inspection). Therefore, silk fabric after SLEP should be sufficiently strong for use. This result is consistent with a visual assessment of the print samples. Furthermore, the advantages of using SLEP are not only the simplicity of the production processes but also that it does not require dye materials.

Furthermore, as a consequence, environmental pollution and the harm to psychological health from its use are eliminated. Thus, SLEP technology could become a new method for forming silk fabric patterns.

Furthermore, yellowing is caused by the radical oxidation of amino acids with aromatic nuclei in fibroin or by the degradation of fibroin peptide chains. Amino acids with aromatic nuclei (yellow) are found in the noncrystallization region. Amino acids that undergo molecular chain breaking are primarily those that occupy a large volume, such as tyrosine, valine, proline, glutamic acid, and threonine<sup>32</sup>. As discussed above, laser printing processes induce unique thermal behaviors<sup>33</sup>. It is assumed that the molecular structures in the proteins are directly damaged. However, because the process is related to the mechanism of molecular pyrolysis, for example, in terms of the strength of thermal action during the printing process, the decomposition process of fibres in silk fabric and its environmental protection property affect the formation of the final materials as well as yellowing and discoloration. The optimization of SLEP parameters should be the subject of further in-depth research.

#### 4 Conclusion

4.1 The carbonized microstructures obtained following SLEP can be divided into bar-shaped clots and sludge materials with small holes. The former are generated by the initial melting of raw silk on the surface of silk fabric; the latter are the combined result of the development of the former along the vertical and horizontal directions and integration during in-depth printing.

4.2 The TG/pyrolysis properties of silk fabric under different atmospheres have been investigated in terms

of the chemical composition and structure of the raw silk. In the TG curves, silk enters a rapid weight loss stage beyond 280°C, and the appearance of a critical point is determined by the composition and structure of raw silk. The pyrolysis speed and extent of weight loss are greatly affected by the heating time and oxygen content. Therefore, printing effects can be achieved by setting reasonable printing parameters.

**4.3 Silk fabric patterns printed by SLEP exhibit yellow chromaticity with 10% lightness, and their boundaries are clear and distinct. Carbonization primarily occurs on the surface of the silk fabric. Due to the high density of the laser energy used, the fibrous proteins of the irradiated silk fabric melt immediately and carbonize at a high temperature regardless of their chemical composition or higher-order structures. Differences are observed in the degree of carbonization of fibrous proteins under different SLEP parameters; however, these differences are not essential distinctions and occur on the surface of the silk fabric. Thus, good printing effects can still be obtained. The technology is feasible and is likely to be developed into a new method for forming silk patterns.**

### Acknowledgement

This work was supported by the Peak of Six Personnel in Jiangsu Province, China (No. 2012-JNHB-013).

### References

- 1 Kothari V K, Sengupta A K, Srinivasan J & Goswami B C, *Text Res J*, 59 (1989) 292.
- 2 Matsumoto Y, Tsuchiya I, Toriumi K & Harakawa K, *Text Res J*, 61 (1991) 131.
- 3 Ke G Z, Xu W L & Yu W D, *Indian J Fibre Text Res*, 33 (2008) 185.
- 4 El-Molla M M, El-Khatib E M, El-Gammal M S & Abdelfattah S H, *Indian J Fibre Text Res*, 36 (2011) 266.
- 5 Venkatraman K, Govindarajan S, Lingasamy K, Balakrishnan M, Thirumanasekaran D & Ramasamy A, *Indian J Fibre Text Res*, 39 (2014) 172.
- 6 Das D, Bhattacharya S, Chandra M & Sankar R, *Indian J Fibre Text Res*, 31 (2006) 559.
- 7 Lundstrom J, Verikas A & Tullander E, *Measurement*, 46 (2012) 1427.
- 8 Chatow U, *Int Conf Digit Print Technol*, (2002) 125.
- 9 Lü F, *Silk*, 49 (2012) 59.
- 10 Wu H H, *Silk*, 49 (2012) 37.
- 11 Qian X P, *Song Brocade Yun Brocade Silk*, 48 (2011) 1.
- 12 Liu A D, Li B & Qiu Y P, *Silk*, 49 (2012) 50.
- 13 Li D, Zhang J Q & Li X J, *Silk*, 49 (2012) 50.
- 14 Zhou Q & Zhao Y C, *J Environ Health*, 22 (2005) 229.
- 15 Cucci I, Boschi A, Arosio C, Bertini F, Freddi G & Catellani M, *Synth Metals*, 159 (2009) 246.
- 16 Chen J X, Wang Y, Xie J, Meng C, Wu G & Zu Q, *Carbohydr Polym*, 89 (2012) 849.
- 17 Xie J, Chen J X, Wang Y, Liu Y F, Noori M N & Pan L, *Cellul Chem Technol*, 48 (2014) 577.
- 18 Chen J X, Xu L N, Xie J, Wang Y, Zu Q & Meng C, *Cellul Chem Technol*, (in press).
- 19 Chantignya M H, Angersa D A & Beauchamp C J, *Soil Biol Biochem*, 32 (2000) 1561.
- 20 Pan L, Chen J X, Wan C F, Ren H, Zhai H M & Wang Y, *Cellul Chem Technol*, (in press).
- 21 Chen J X, Pan L, Xie J, Wu G, Ren H & Wang Y, *Cellulose* 21 (2014) 2871.
- 22 Chen J X, Xie J, Pan L, Wang X, Xu L N & Lu Y, *J Wood Chem Technol*, 34 (2014) 202.
- 23 Wu C Y, Feng Z Z, Wan S M & Wu J Y, *Silk Chemistry*, 2nd edn. (China Textile Press, Beijing), 1990, 6-90.
- 24 Zuo B Q, Zha M & Yang Y M, *Silk*, 40 (2003) 35.
- 25 Sashina E S, Janowska G, Zaborski M & Vnuchkin A V, *J Therm Anal Calorim*, 89 (2007) 887.
- 26 Wu S Q, Li M Y, Fang B S & Tong H, *Carbohydr Polym*, 88 (2012) 496.
- 27 Zhang H, Magoshi J, Becker M, Chen J Y & Matsunaga R, *J Appl Polym Sci*, 86 (2002) 1817.
- 28 Freddi G, Tsukada M & Beretta S, *J Appl Polym Sci*, 71 (1999) 1563.
- 29 Liu G F, Wang X L & Hu C, *J Zhejiang Sichou Inst Technol* 10 (1993) 1.
- 30 Luo W Z & Feng Y F, *J Zhejiang Sichou Inst Technol*, 7 (1990) 52.
- 31 Wray L S, Hu X, Gallego J, Georgakoudi I, Omenetto FG, Schmidt D & Kaplan D L, *J Biomed Mater Res B*, 99 (2011) 89.
- 32 Reddy N & Yang Y Q, *J Mater Sci*, 45 (2010) 6617.
- 33 Chen J B & Peng R L, *The Theory and Application of Laser* (Electronic Industry Press, Beijing), 2010, 163-166.